

## CHARACTERIZATION AND ELECTRICAL PROPERTIES OF DOPED SrTiO<sub>3</sub> CERAMICS

T. SOFI SARMASH, K. CHANDRA BABU NAIDU, P. SANDHYA & T. SUBBARAO

Department of Physics, Material Science Lab, S. K. University, Anantapur, Andhra Pradesh, India

### ABSTRACT

Pure, manganese and zinc doped SrTiO<sub>3</sub> ceramic powder particles were synthesized via conventional solid state route diffusion method. After ball milling, these samples were calcined at 1250<sup>0</sup>C, 1050<sup>0</sup>C and 1050<sup>0</sup>C for 9hr, 8hr and 8hrs respectively. Further these pellets were sintered at 1300<sup>0</sup>C, 1250<sup>0</sup>C and 1250<sup>0</sup>C for 4hr, 2hr and 2hrs respectively. Subsequently the samples were characterized using XRD, SEM and EDAX for the elucidation of structural, surface morphological and elemental respectively. The average crystalline sizes were accomplished as 28.14nm, 40.85nm and 98.73nm respectively and lattice parameters were calculated as 3.9541Å<sup>0</sup>, 3.903 Å<sup>0</sup> and 4.8702 Å<sup>0</sup> respectively using X-Ray diffraction spectra. Apart from these DC-activation energies were computed using lnσ Vs 1/T plots. The average grain sizes were calculated as 1.41μm, 1.15μm and 1.65 μm respectively from Scanning Electron Microscopy images.

**KEYWORDS:** X-ray Diffract Meter, Scanning Electron Microscopy, FTIR, Solid State Route Method, AC-Conductivity

### INTRODUCTION

SrTiO<sub>3</sub> is an ABO<sub>3</sub> perovskite structured material and exhibits excellent optical transparent properties in visible region and therefore it is being used as a candidate material in optoelectronic devices<sup>1</sup>. At room temperature strontium titanate exhibits cubic structure and at approximately 110K the structure was changed from cubic to tetragonal<sup>2</sup>. Manganese doped SrTiO<sub>3</sub> revealed a single cubic perovskite phase similar to SrTiO<sub>3</sub> and second phase peaks begin to appear in the XRD structure which are suitable to the peaks of MnTiO<sub>3</sub> with increase of Mn content in the lattice site of SrTiO<sub>3</sub><sup>3</sup>. The average grain size of Mn doped SrTiO<sub>3</sub> doesn't depend upon the concentration Mn content but depends on the sintering conditions. AC-Conductivity studies of Mn doped SrTiO<sub>3</sub> revealed that ac-conductivity is increasing with increase of temperature due to the hopping mechanism and the activation energies E<sub>a</sub> = 0.068eV, 0.087eV and 0.079eV when τ<sub>0</sub> = 2.1×10<sup>-14</sup>s, 0.8×10<sup>-14</sup>s and 0.7×10<sup>-14</sup>s were carried out using Cole-Cole equation and Arrhenius law τ = τ<sub>0</sub> exp (-E<sub>a</sub>/KT)<sup>4</sup>. The increase in the activation energy is due to increase of the concentration of polar dipoles and because of intensification of dipole interaction through the phonons of SrTiO<sub>3</sub> lattice<sup>4</sup>. ZnO is an excellent material for having outstanding optical and electronic properties like wide band gap round about 3.37 eV<sup>5-6</sup>. Zn doped SrTiO<sub>3</sub> and pure SrTiO<sub>3</sub> expressed the band gap of 3.2eV in its UV-Visible absorption spectra and it exhibits photo catalytic activity<sup>7-8</sup>. In this investigation the author is intended to study DC-Conductivity properties along with XRD, SEM and EDAX analysis.

### PREPARATION OF THE SAMPLES

In order to synthesize the pure, Mn and Zn doped SrTiO<sub>3</sub> ceramic powder particles SrCO<sub>3</sub> (99.5% purity), TiO<sub>2</sub> (99.5% purity), MnO<sub>2</sub> (99.5% purity) and ZnO (99.5% purity) were taken as the raw materials. In these materials initially to prepare pure SrTiO<sub>3</sub>, Mn and Zn doped SrTiO<sub>3</sub> ceramic powders, (SrCO<sub>3</sub>, TiO<sub>2</sub>), (SrCO<sub>3</sub>, MnO<sub>2</sub>, TiO<sub>2</sub>) and (SrCO<sub>3</sub>, ZnO, TiO<sub>2</sub>) were weighed and mixed in their Stoichiometric ratio. Furthermore these were ball milled for nearly 20hr, 16hr and 12hr respectively. After wards samples were calcined at 1250<sup>0</sup>C, 1050<sup>0</sup>C and 1050<sup>0</sup>C for 9hr, 8hr and 8hrs respectively. Further the pellets were sintered at 1300<sup>0</sup>C, 1250<sup>0</sup>C and 1250<sup>0</sup>C for 4hr, 2hr and 2hrs respectively. Pellets were cooled to

room temperature at the rate of  $5^{\circ}\text{C}/\text{min}$ . and these were coated with silver paste on either side of the pellets without contacting the corners. Later samples were characterized using XRD, SEM, EDAX and HIOKI 3532-50 LCR HiTESTER for the elucidation of structural, surface morphological, elemental and dc-conductivity properties respectively.

## RESULTS AND DISCUSSIONS

### XRD Analysis

XRD technique is used to determine the structure of compound and in the present investigation Pure, manganese and zinc doped  $\text{SrTiO}_3$  structures have been revealed as cubic. Lattice parameters were found as  $3.9541\text{\AA}$ ,  $3.903\text{\AA}$  and  $4.8702\text{\AA}$  ( $a=b=c$ ) for  $\text{SrTiO}_3$ ,  $\text{Sr}_{0.5}\text{Mn}_{0.5}\text{TiO}_3$  and  $\text{Sr}_{0.5}\text{Zn}_{0.5}\text{TiO}_3$  respectively and are in consistent with standard values in literature<sup>9, 3, 10</sup>. From XRD profile (h k l) value were calculated as (100),(110),(111),(200),(210),(211),(220) and (310).Furthermore the average crystalline sizes(28.145nm,40.85nm and 98.73nm) using Scherer equation ( $D_p$ ),average dislocation densities ( $138\times 10^{13}\text{m}^{-3}$ ,  $601\times 10^{12}\text{m}^{-3}$  and  $842\times 10^{12}\text{m}^{-3}$ ) and average elastic strains (0.1725,0.2646 and 0.2693) were established for ST, Mn and Zn doped ST respectively using the following formula. As the crystalline size is nano this depresses the calcination and sintering temperatures of the specimen<sup>11</sup>.

$$D_p = K \lambda / \beta \cos\theta, \rho = 1/D^2 \text{ and } E_{\text{strain}} = \beta/4\tan\theta$$

Where K is a constant and is equal to 0.9 &  $\lambda=0.15418\text{ nm}$  ( $\text{CuK}_\alpha$ ),  $\beta$  is full width half maxima

As just described in Andrei L.Kholkin et al<sup>3</sup> XRD profile of  $\text{Sr}_{1-x}\text{Mn}_x\text{TiO}_3$  at  $x=0$  the phases are consistent with undoped strontium titanate and up to  $x<0.10$  there is no second phase appearance except single phase but mean while i.e.  $x\geq 0.10$  SMnT showed some second phases starting to appear which are consistent with  $\text{MnTiO}_3$  phases. On the other hand the XRD profile of  $\text{SrTi}_{1-y}\text{Mn}_y\text{O}_3$  showed a cubic structure without having any second phases for various concentrations of manganese at  $x\leq 0.15$ .In this investigation at  $x=0.5$  the XRD profile was carried out and exhibited some second phases along with single phase structure. It is confirmed that the specified(star symbol) phases in following XRD are due to presence of  $\text{MnTiO}_3$  and this explicitly establishes a fact that formation of second phases depend upon the occupation of manganese into the site of ST. In  $\text{Sr}_{0.5}\text{Zn}_{0.5}\text{TiO}_3$  ceramics also some second phase structures have been appeared and were consistent with  $\text{ZnTiO}_3$  phases. More over due to presence of two impurities (Mn and Zn) the resultant structure was not changed from cubic to any other structure. Due to the presence of second phases in XRD the compound loses its good properties such as optical, dielectric, photo catalytic, thermoelectric and conductivity properties etc.

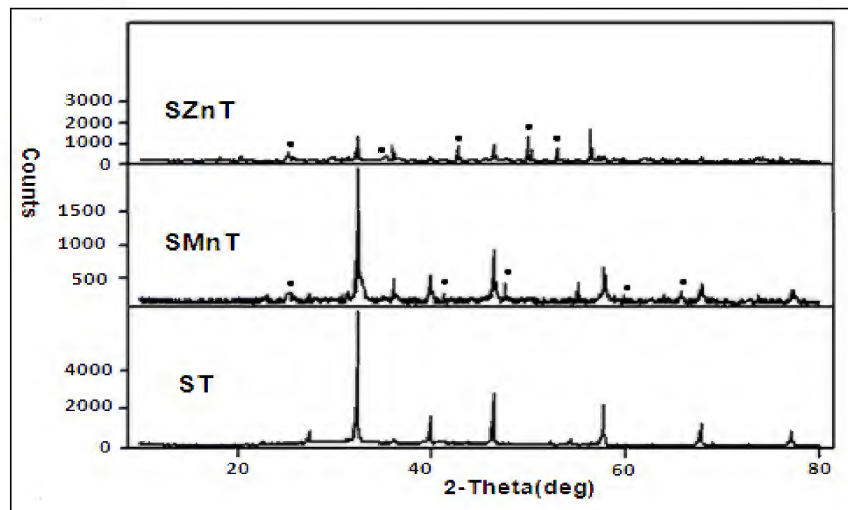


Figure 1: XRD Results of Pure  $\text{SrTiO}_3$  (ST),  $\text{Sr}_{0.5}\text{Mn}_{0.5}\text{TiO}_3$  (SMnT) and  $\text{Sr}_{0.5}\text{Zn}_{0.5}\text{TiO}_3$  (SZnT) Ceramics

### SEM and EDAX Analysis

Scanning electron microscopy is used effectively in micro analysis and failure analysis of solid materials. This approach is useful in qualitatively or semi-quantitatively determining chemical compositions, crystalline structure and crystal orientations. The following SEM figures are made at the different spots having different magnifications and in 5  $\mu\text{m}$ , 3  $\mu\text{m}$  range. In the SEM images few dislocations and grains along with grain boundaries have been observed. The average grain sizes ( $G_a$ ) of SrTiO<sub>3</sub>, Sr<sub>0.5</sub>Mn<sub>0.5</sub>TiO<sub>3</sub> and Sr<sub>0.5</sub>Zn<sub>0.5</sub>TiO<sub>3</sub> calculated as 1.41  $\mu\text{m}$ , 1.15  $\mu\text{m}$  and 1.65  $\mu\text{m}$  respectively using the following formulae.

Average grain size  $G_a = 1.5 L/MN$ , Where L=the total test line length, M=the magnification,

N=the total number of intercepts which the grain boundary makes with the line.

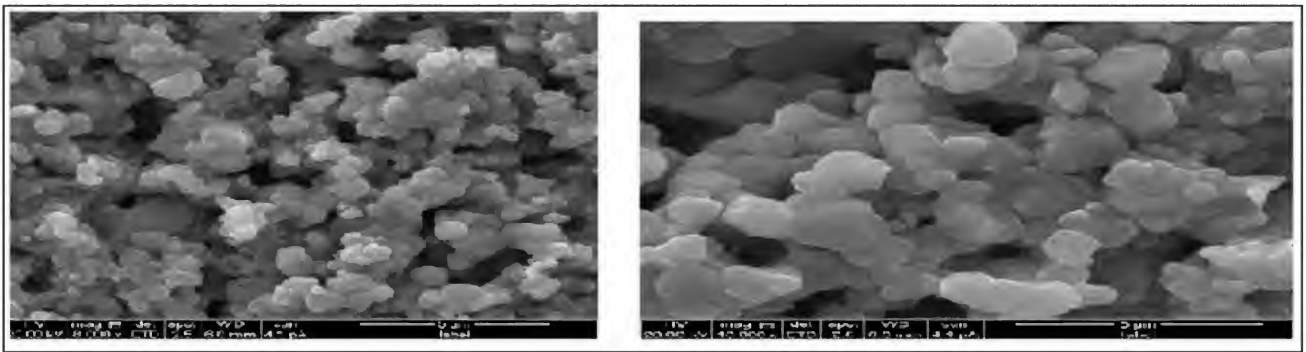


Figure 2: SEM Images of Undoped SrTiO<sub>3</sub> Ceramics

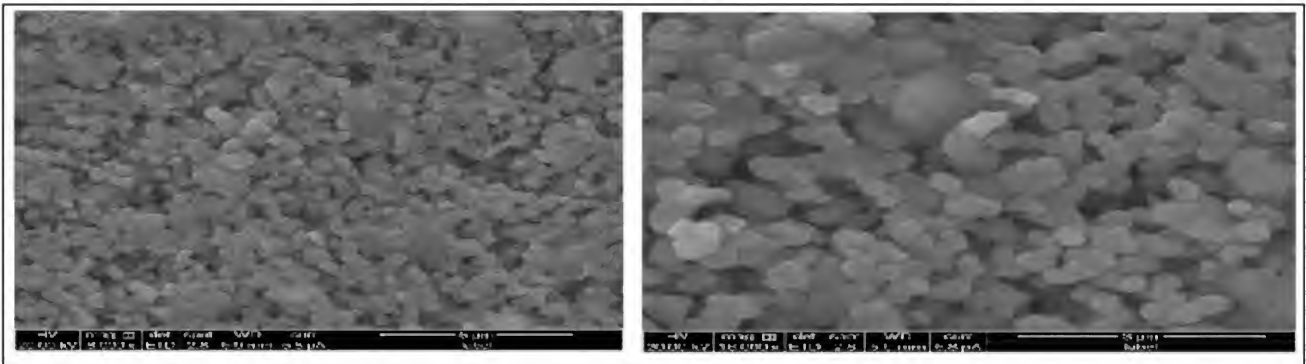


Figure 3: SEM Images of Sr<sub>0.5</sub>Mn<sub>0.5</sub>TiO<sub>3</sub> Ceramics

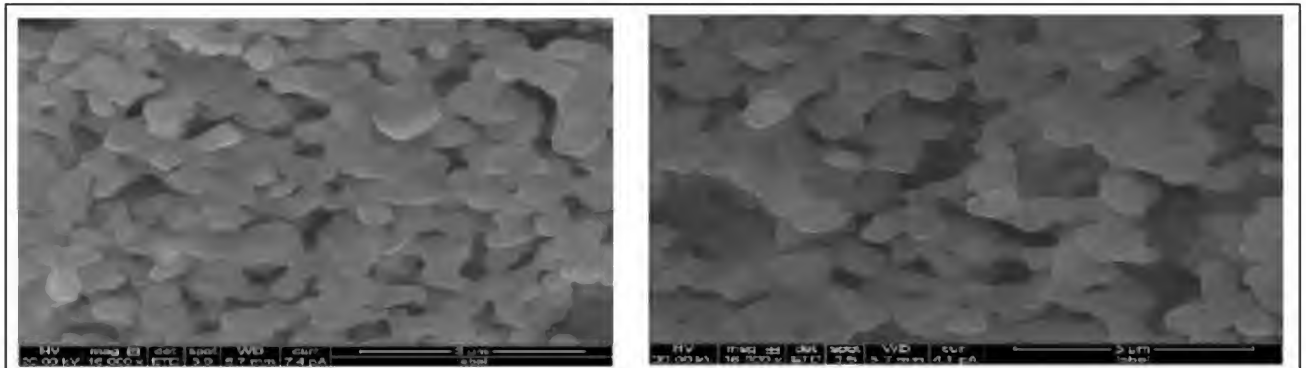


Figure 4: SEM Images of Sr<sub>0.5</sub>Zn<sub>0.5</sub>TiO<sub>3</sub> Ceramics

It is obvious from the SEM images of SrTiO<sub>3</sub>, Sr<sub>0.5</sub>Mn<sub>0.5</sub>TiO<sub>3</sub> and Sr<sub>0.5</sub>Zn<sub>0.5</sub>TiO<sub>3</sub> that the grain growth is high for ST while lower grain growth is observed for SMnT and SZnT ceramics. This due to the fact of sintering temperature of pellets<sup>12</sup>

An EDAX detector is used to separate the characteristic X-rays of different elements into an energy spectrum and EDAX system software is used to analyze the energy spectrum in order to determine the abundance of specific elements. The following image shows the elements present in sample and their concentrations. In the following EDAX images the elements present in the compounds with their concentrations were shown.

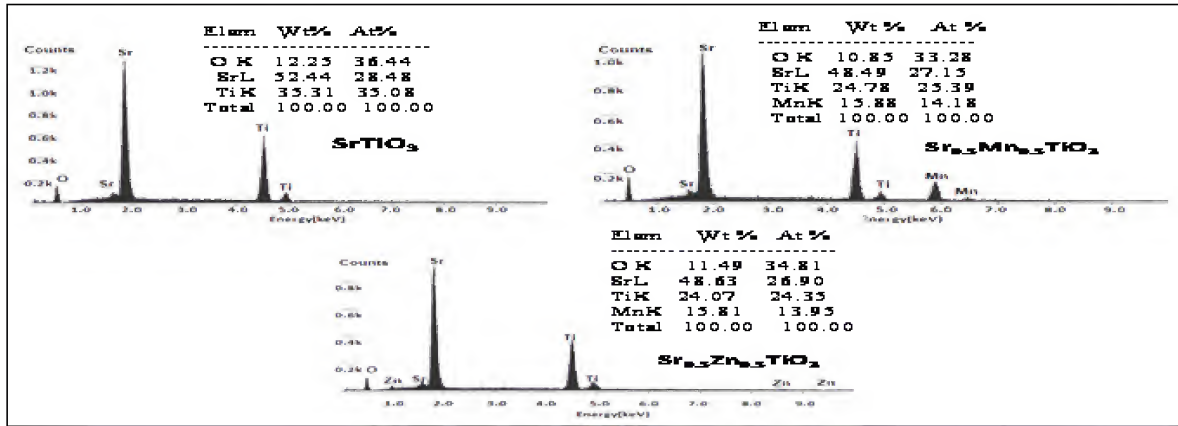


Figure 5: EDAX Images of Pure  $\text{SrTiO}_3$ ,  $\text{Sr}_{0.5}\text{Mn}_{0.5}\text{TiO}_3$  and  $\text{Sr}_{0.5}\text{Zn}_{0.5}\text{TiO}_3$  Ceramics

## DC-CONDUCTIVITY

DC-conductivity of  $\text{SrTiO}_3$ ,  $\text{Sr}_{0.5}\text{Mn}_{0.5}\text{TiO}_3$ , and  $\text{Sr}_{0.5}\text{Zn}_{0.5}\text{TiO}_3$  ceramics were performed using HIOKI 3532-50 LCR HiTESTER at a fixed frequency of 100Hz. DC-conductivity of  $\text{SrTiO}_3$ , is increasing with increase of temperature up to 350K due to electro static interaction between a conduction electron or hole which results in displacement of nearby ions and later decreases up to 425K due to decrease of electro static interaction which causes to decrease of hopping mechanism. For further temperatures due to linear hopping mechanism dc-conductivity goes on increasing. This kind of activated hopping mechanism i.e. for the process of jumping of carriers, the mobilities are found to be proportional to  $-E/K_B T$  and from Heikes and Johnson expression for conductivity<sup>13</sup> the activation energies were computed as 0.9484eV, 0.9624 eV and 0.9579 eV for  $\text{SrTiO}_3$ ,  $\text{Sr}_{0.5}\text{Mn}_{0.5}\text{TiO}_3$ , and  $\text{Sr}_{0.5}\text{Zn}_{0.5}\text{TiO}_3$  ceramics. This establishes a fact that there is no considerable variation of activation energies of the three samples. The increasing and decreasing behavior of dc-conductivity and  $\ln \sigma_{dc}$  with reference to the temperature and  $1000/T$  were clearly described in the following plots.

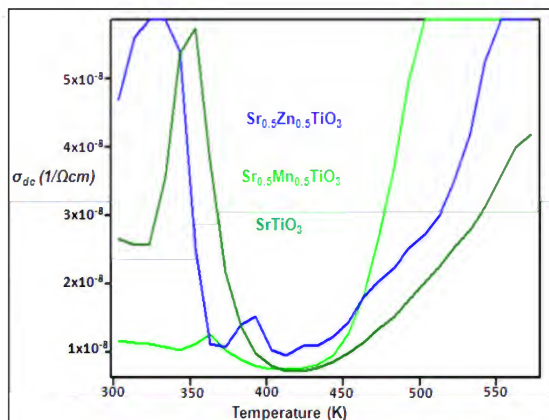


Figure 6:  $\Sigma_{dc}$  vs Temperature Plots

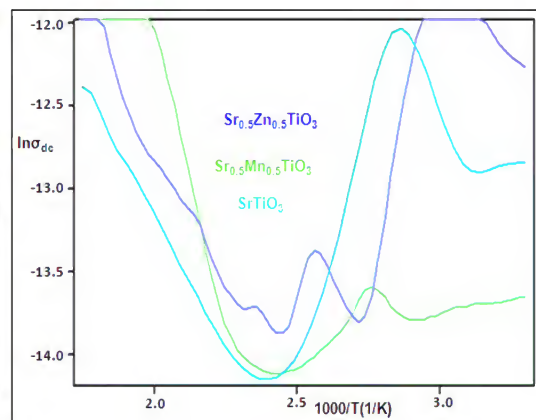


Figure 7:  $\ln \sigma_{dc}$  Vs  $1000/T$  Plots

## CONCLUSIONS

In XRD spectra the formation of single phase structures of Mn and Zn doped strontium titanate depend upon the dopant site occupancy. There is no obvious difference among the pure, Mn and Zn doped Strontium titanate in the

crystalline surface morphology characteristics except variation of grain growth which is a temperature dependent parameter and XRD peak positions with an exception of few specified second phases due to increase of concentrations of dopants.

## ACKNOWLEDGEMENTS

This work was financially supported by a project of University Grants Commission (UGC)-NEW DELHI, INDIA. Also thanks to Vellore Institute of Technology (VIT), Tamilanadu, and IISC-Bangalore for supporting in characterization works such as XRD and SEM of my samples and giving their valuable suggestions.

## REFERENCES

1. D. Karim, S. Aisahmat, R. Hussin, W. Nurulhuda, W. Shemsuri, I. Bakar and I. Zunhairi UMT 11<sup>th</sup>
2. *International Annual Symposium on sustainability science and management*, 9<sup>th</sup>-11<sup>th</sup> July 2012, Jarengann, Malaysia.
3. Fleury PA, Scott JF, Worlock JM. *Phys. Rev. Lett.*, (1968); 21:16.
4. Alexander Tkach, Paula M. Vilarinho, Andrei L. Kholkin, *Acta materialia*, 53(2005) 5061-5069.
- a. Tkach, P.M. Vilarinho, A.L. Kholkin. *Acta materialia*, 54(2006) 5385-5391
5. Look DC. *Mater. Sci. Eng B.*, (2001); 80:383-7.
6. Ozguc U, Aliviy YI, Liu C, Teke A, Reshchikov MA, Dogan [S], et al. *J. Appl. Phys.*, (2005); 98:141301.  
WANG Gui-yun, QIN Ya, CHENG Jie, WANG Yan-ji\* *J. Fuel Chem. Technol.*, (2010), 38(4), 502-507.
7. Mittal, Manish; Sharma, Manoj; Pandey, *Journal of Nano Science and Nano technology* O.P. pp. 2725-2733(9),(2014)
8. R. H. Mitchell, A. R. Chakhmouradian, P. M. Woodward, *Physics and Chemistry of Minerals*, 27(2000)583.
9. K. Chandra Babu Naidu, T. Sofisarmash and T. Subbarao, *International Journal of Scientific & Engineering Research*. 1342- 1346, (2014), ISSN 2229-5518,
10. T Bachel, H-J Gunterodt and R Schafer, *Phys. Rev. Lett.*, 85, 1250 (2000).
11. Bhuiyan, Mahabub Alam, Choudhury, Shamima, *Journal of Bangladesh Academy of Sciences.*, Vol. 34, No. 2, 189-195, (2010).
12. R. R. Heikes and W. D. Johnson, *J. Chem. Phys.*, 26 (1957) 582

